

# Translational dynamics of water in the nanochannels of oriented chrysotile asbestos fibers

E. Mamontov,<sup>1,2</sup> Yu. A. Kumzerov,<sup>3</sup> and S. B. Vakhrushev<sup>3</sup>

<sup>1</sup>*NIST Center for Neutron Research, National Institute of Standards & Technology, 100 Bureau Drive, MS 8562, Gaithersburg, Maryland 20899-8562, USA*

<sup>2</sup>*Department of Materials Science and Engineering, University of Maryland, College Park, Maryland 20742-2115, USA*

<sup>3</sup>*Ioffe Physico-Technical Institute, 194021 St. Petersburg, Russia*

(Received 3 December 2004; revised manuscript received 14 February 2005; published 7 June 2005)

We performed a high-resolution quasielastic neutron scattering study of water dynamics in fully hydrated oriented chrysotile asbestos [chemical formula  $\text{Mg}_3\text{Si}_2\text{O}_5(\text{OH})_4$ ] fibers. The fibers possess sets of macroscopically long, parallel channels with a characteristic diameter of about 5 nm. Freezing of water in the channels was observed at about 237 K. Measurements at 280, 260, and 240 K revealed a translational dynamics of water molecules with the relaxation time slower by more than an order of magnitude compared to bulk water. The  $Q$  dependence of the quasielastic broadening was typical of a translational diffusion motion with a distribution of jump lengths, similar to that observed in bulk water. The relaxation time showed no significant anisotropy in the measurements with the scattering vector parallel and perpendicular to the fiber axes.

DOI: 10.1103/PhysRevE.71.061502

PACS number(s): 61.12.Ex, 68.08.-p

## I. INTRODUCTION

Because of the exceptionally large incoherent scattering cross section of hydrogen compared to other elements, neutron scattering is an attractive technique for studying the dynamics of water confined within various nanoporous structures. Quasielastic neutron scattering (QENS) studies of water molecules motions benefit from the fact that the wavelength of a cold neutron is comparable with a typical diffusion jump distance. Thus, the dependence of the quasielastic scattering on the scattering momentum transfer,  $Q$ , may yield information on the nature of the diffusion jumps of water molecules.

Most of the QENS studies of the behavior of water in confinement are performed using hosts that possess a three-dimensional porous structure, either regular, such as zeolites [1] and mesoporous silica [2–6], or irregular, such as vycor glass [7–9] and porous gels [10]. Examples of quasi-two-dimensional systems include interlayer water in clays [11–16] and surface water in oxides [17,18]. Several ongoing studies involve quasi-one-dimensional water in nanotubes. The diameters of single-wall nanotubes range between 1 and 2 nm, and the average length may be several micrometers. In this work, we studied the dynamics of water in chrysotile asbestos fibers. While the diameter of channels in the fibers is a few nanometers, the fiber length may be 1 cm or higher. The nanochannels in bundles of chrysotile asbestos fibers not only have a very high aspect ratio, but also, unlike carbon nanotubes, are aligned macroscopically. This provides an interesting opportunity to study anisotropy of the dynamics of confined water.

The morphology of chrysotile asbestos [chemical formula  $\text{Mg}_3\text{Si}_2\text{O}_5(\text{OH})_4$ ] consists of parallel, closely packed tubes with typical inner and outer diameters of 2–8 and 20–40 nm, respectively (see Fig. 1). Their crystal structure consists of layers of partially hydrated MgO bound to a corresponding  $\text{SiO}_2$ . The crystal structure of chrysotile was studied extensively by Whittaker using x-ray diffraction [19]. The micro-

structure of chrysotile fibers was investigated by Yada using high-resolution electron microscopy [20,21]. Pundsack [22] studied the porous structure of blocks of chrysotile fibers. In agreement with the results of electron microscopy, he concluded that the interfiber channel size in the close-packed bundles of fibers was comparable to the intrafiber channel size, and the total pore volume ranged from 4% to 5% of the sample volume. Recently, there has been a revived interest in chrysotile asbestos because of its potential suitability for nanowire preparation (see Ref. [23] for a summary of experiment results and discussion).

We performed a high-resolution QENS study of water dynamics in fully hydrated chrysotile asbestos. The freezing point of water in chrysotile asbestos was found to be suppressed to about 237 K. The translational motion of water molecules was observed at 280, 260, and 240 K. The relaxation time showed no significant anisotropy in the measurements with the scattering vector parallel and perpendicular to the fiber axes. The  $Q$  dependence of the quasielastic broadening was typical of a translational motion with a distribution of jump lengths, similar to that observed in bulk water [24]. However, the relaxation times exceeded those for translational motion in bulk water by more than an order of magnitude.

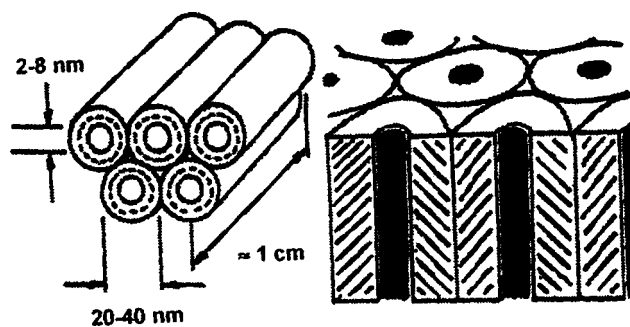


FIG. 1. A schematic picture of a bundle of chrysotile asbestos fibers.

## II. EXPERIMENT

Chrysotile asbestos fibers with an average outer and inner diameter of 28 nm and 5 nm, respectively, were obtained from the collection of Ioffe Physico-Technical Institute, St Petersburg, Russia. The macroscopic bundles of fibers had a cross section of up to  $1 \times 2 \text{ mm}^2$  and a length of up to 1.5 cm. Prior to the filling with water, the fiber bundles were evacuated at 383 K, and their mass was determined to be 2.8812 g. The fibers were then filled with water by means of submerging for several days and subsequent drying at 313 K in the air. The water uptake calculated as the mass difference between the hydrated and dried sample and the sample after evacuation was 0.0928 g. This corresponds to 1 water molecule per 2 molecules of  $\text{Mg}_3\text{Si}_2\text{O}_5(\text{OH})_4$ . For the water adsorbed only in the 5 nm intrafiber channels, the maximum uptake of about 1  $\text{H}_2\text{O}$  molecule per 5 molecules of  $\text{Mg}_3\text{Si}_2\text{O}_5(\text{OH})_4$  can be expected based on the chrysotile density of  $2.56 \text{ g/cm}^3$  and water density of  $1 \text{ g/cm}^3$ . The high level of hydration is thus indicative of the water absorption in both the intra- and interfiber channels. For the ideal hexagonal close packing of fibers with the dimensions as studied in our experiment, the cross section of the interfiber channels is 60% larger than that of the intrafiber channels, and there are twice as many interfiber channels as there are intrafiber channels. However, the outermost surface of fibers is highly irregular, and the interfiber channels may be partially or fully filled with amorphous material, thus greatly reducing the channel cross section.

The bundles of fibers were placed together onto a thin aluminum foil so that their axes were aligned and the bundles made up a single layer with a thickness of about 1 mm over half of the foil. The foil was then folded forming a “flat plate” of bundles of fibers with the same direction of axes and securely placed into a thin aluminum sample holder. The sample holder was sealed with an indium O ring and mounted onto a closed-cycle refrigerator. The temperature was controlled to within  $\pm 0.5 \text{ K}$ .

QENS experiments were carried out using the high-flux backscattering spectrometer (HFBS) at the National Institute of Standards and Technology (NIST) Center for Neutron Research [25]. In the standard operation mode of the spectrometer, the incident neutron wavelength is varied via Doppler shifting about a nominal value of  $6.271 \text{ \AA}$  ( $E_0 = 2.08 \text{ meV}$ ). After scattering from the sample, only neutrons having a fixed final energy of 2.08 meV are measured by the detectors, as ensured by Bragg reflection from analyzer crystals. When operated with a dynamic range of  $\pm 35 \mu\text{eV}$ , the full width of the instrument resolution function at half maximum is about  $1.20 \mu\text{eV}$ . The spectra collected at  $0.25 \text{ \AA}^{-1} < Q < 1.42 \text{ \AA}^{-1}$  (at the elastic channel) at 280, 260, and 240 K were used in the data analysis. In addition, the spectrum collected at 100 K was used to determine the sample geometry-dependent resolution function. In the alternative operation mode of the spectrometer called the fixed-window mode, the Doppler drive was stopped, and only the elastic scattering intensity was collected while the sample temperature was ramped down from 300 to 100 K at a rate of  $0.5 \text{ K/min}$ . The energy resolution of the HFBS in this mode of operation is about  $0.8 \mu\text{eV}$ . The fixed-window mode is

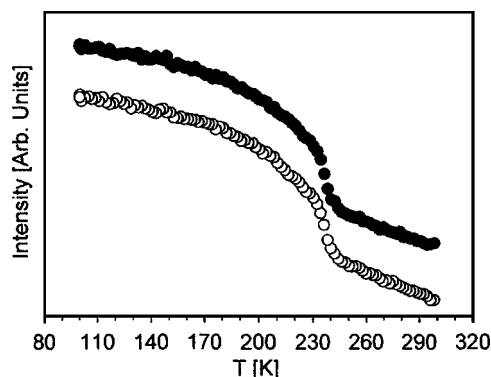


FIG. 2. The elastic scattering intensity measured in the fixed-window mode as a function of temperature and summed up over all  $Q$  values. Open circles: “ $Q$ -parallel” orientation. Filled circles: “ $Q$ -perpendicular” orientation. An arbitrary vertical offset of the baselines is applied for clarity. The increase in the elastic scattering at about  $T = 237 \text{ K}$  is due to the freezing of water in the fibers.

especially useful for studying phase transitions such as freezing or melting.

All the measurements reported in this paper were performed with two different orientations of the “flat plate” made of the bundles of fibers with respect to the scattering vector. In the first orientation, the fibers made a  $45^\circ$  angle to the incident beam in order to make the elastic  $Q$  vector parallel to the axes of fibers for the scattering angle of  $90^\circ$  ( $Q = 1.42 \text{ \AA}^{-1}$ ). The elastic  $Q$  vectors for the other scattering angles had nonzero projections onto the directions of the fiber axes. Throughout the paper, we depict the data obtained in this geometry with open symbols, and, for the sake of simplicity, call this geometry “ $Q$  parallel.” The second orientation was obtained from the first one by means of rotating the sample by  $90^\circ$  about the axis perpendicular to the “flat plate” in the horizontal plane. In this orientation, the elastic  $Q$  vectors for all scattering angles are perpendicular to the fiber axes. The data obtained in this geometry are depicted with filled symbols, and the geometry is called “ $Q$  perpendicular.”

## III. RESULTS AND DISCUSSION

The elastic scattering intensities measured as a function of temperature in the course of cooling down and summed up over all  $Q$  values are presented in Fig. 2. The data clearly show an abrupt increase in the elastic scattering due to the freezing of water at about 237 K. The suppression of the freezing temperature of water in confined geometry has been well known [2,3,26–29]. The onset of freezing of water in the chrysotile nanochannels at 237 K is in good agreement with the data available in the literature (252 K and 237 K in silica with the average pore size of 10 nm and 3 nm, respectively [2], 260 K in 9 nm silica pores [26], 242 K and 221 K in 1.87 nm and 1.44 nm MCM-41 [3], 232 K in 4.2 nm MCM-41 [28], and 255 K in vycor glass with the average pore size of 5 nm [27]). No significant difference between the freezing temperatures obtained in the “ $Q$ -parallel” and “ $Q$ -perpendicular” orientations could be observed, and an ar-

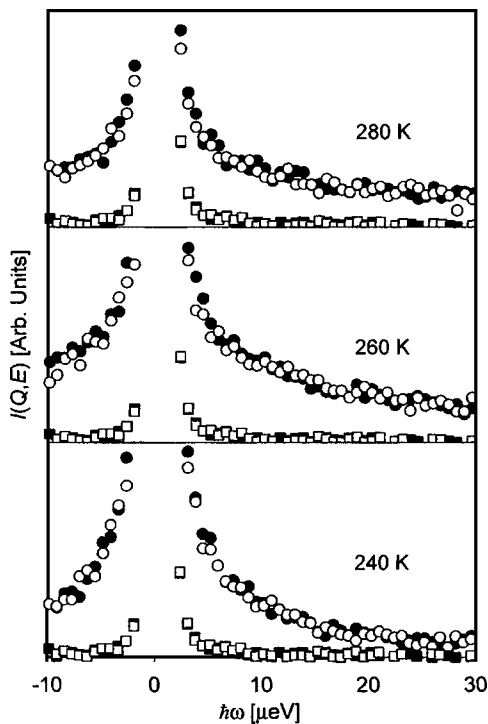


FIG. 3. The scattering intensities measured in the energy space at the  $90^\circ$  detector ( $Q=1.42 \text{ \AA}^{-1}$ ). The elastic peaks at zero energy transfer are truncated to better demonstrate the quasielastic signal. The 100 K data used as a resolution function are plotted on every graph and shown with squares. Open symbols: “ $Q$ -parallel” orientation. Filled symbols: “ $Q$ -perpendicular” orientation.

bitrary vertical offset of the baselines had to be applied in Fig. 2 in order to avoid an excessive overlap of the plots.

The scattering intensities measured at the  $90^\circ$  detector ( $Q=1.42 \text{ \AA}^{-1}$ ) at three temperatures are shown in Fig. 3 along with the data collected at 100 K. The latter represents the resolution function. The quasielastic signal narrows as the temperature is decreased, indicating slower motion of water molecules. We fit the data with the expressions that include a single Lorentzian with half-width at half-maximum,  $\Gamma(Q)$ , for the quasielastic broadening,

$$I(Q, \hbar\omega) = C(Q)\{x(Q)\delta(\hbar\omega) + [1 - x(Q)]L(Q, \hbar\omega) + A_1\hbar\omega + A_2\} \otimes R(Q, \hbar\omega), \quad (1)$$

$$L(Q, \hbar\omega) = \frac{1}{\pi} \frac{\Gamma(Q)}{(\hbar\omega)^2 + \Gamma^2(Q)}. \quad (2)$$

Here  $C(Q)$  is a scaling constant,  $x(Q)$  is the fraction of the elastic scattering,  $R(Q, \hbar\omega)$  is the resolution function in the energy space, and  $L(Q, \hbar\omega)$  is a Lorentzian relaxation function for water molecules. The linear background term,  $A_1\hbar\omega + A_2$ , accounts for the inelastic scattering on a much faster time scale compared to the dynamic range of the back-scattering spectrometer. The elastic scattering is due to immobile atoms (mostly hydrogen) in both the structural hydroxyl groups in  $\text{Mg}_3\text{Si}_2\text{O}_5(\text{OH})_4$  and possibly the OH/ $\text{H}_2\text{O}$  layer in direct contact with the surface of channels. Attempts

to fit the data using an expression for the elastic broadening that incorporates more than one Lorentzian to account for both slower translational and faster rotational diffusion components [18,30] have not improved the fit, which suggests that the rotational component of the water diffusion in chrysotile asbestos is too fast for the dynamic range of the instrument ( $\approx 20$  ps) in the temperature range studied, and probably contributes to the background. This is not unexpected based on the numerous previous findings that the translational diffusion component for water in confinement slows down dramatically compared to bulk water, often by an order of magnitude or more, whereas the rotational component slows down by a factor of 2–3 only. For bulk water in the temperature range of 253–293 K, the relaxation time for the rotational component  $1 \text{ ps} < \tau < 2 \text{ ps}$  has been reported [24]. We were unable to fit the data at the lowest  $Q$  value for the 240 K dataset using Eqs. (1) and (2), probably because the quasielastic broadening was too small for the spectrometer resolution of  $1.20 \mu\text{eV}$ .

Importantly, we observe no pronounced anisotropy between the data collected in the “ $Q$ -parallel” and “ $Q$ -perpendicular” geometries not only at the  $90^\circ$  detector shown in Fig. 3, but also at all the other detectors. This suggests that the  $Q$  dependence of the Lorentzian quasielastic broadening should follow a law for the powder-averaged systems [31]. A translational motion of water molecules that is much faster along the fiber axes than in the directions perpendicular to the axes would manifest itself in a significant difference in quasielastic signals measured in the “ $Q$ -parallel” and “ $Q$ -perpendicular” geometries. In the limit when the motions take place along the fiber axes only, there would be no quasielastic broadening in the “ $Q$ -perpendicular” geometry, while in the “ $Q$ -parallel” geometry the  $Q$  dependence of the Lorentzian quasielastic broadening would not follow a powder-averaged law. However, as one can see in Fig. 4, the  $Q$  dependence of the parameter  $\Gamma(Q)$  for both sample orientations can be approximately described by the powder-averaged law for a jump diffusion model with an exponential distribution of jump lengths,  $P(r) = (r/r_0^2)\exp(-r/r_0)$  [31,32],

$$\Gamma(Q) = \frac{\hbar}{\tau_{res}} \left[ 1 - \frac{1}{1 + \frac{Q^2 \langle r^2 \rangle}{6}} \right], \quad (3)$$

where  $\tau_{res}$  is the residence time between jumps. The values of  $\tau_{res}$  are summarized in Table I [33]. While the residence time obtained at 280 K exceeds that obtained at 260 K, suggesting that using Eqs. (1)–(3) for data analysis may be just a crude approximation, it is clear that the residence time shows no significant anisotropy between the two sample orientations. For comparison, the residence time between jumps for the translation component of diffusion in bulk water is 1.25 ps at 293 K, 2.33 ps at 278 K, and 7.63 ps at 261 K [24]. Thus, we observe a very substantial slowing down of the translational motions compared to bulk water. As we discussed above, the rotational component of the diffusion could not be resolved, which suggests that, even if it slows down compared to the bulk water values of 1–2 ps, it still

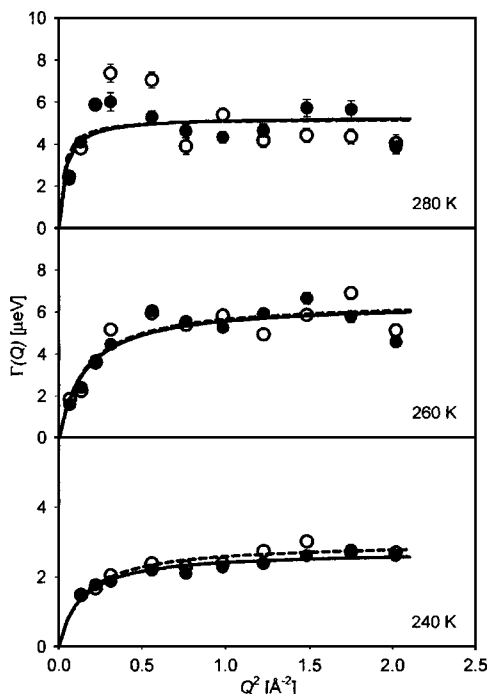


FIG. 4. The  $Q$  dependence of the parameter  $\Gamma(Q)$  obtained from fitting the data using Eqs. (1) and (2) and its fit with Eq. (3). Open circle data points and dashed line fitting curves: “ $Q$ -parallel” orientation. Filled circle data points and solid line fitting curves: “ $Q$ -perpendicular” orientation.

remains much faster than  $\approx 20$  ps, the dynamic range of the backscattering spectrometer.

As pointed out above, one would expect a very significant anisotropy of the quasielastic broadening between the “ $Q$ -perpendicular” and “ $Q$ -parallel” orientations for the water molecules moving primarily along the fiber axes. On the contrary, our results demonstrate almost isotropic picture of translational motions of the water molecules in chrysotile asbestos fibers with a characteristic channel size of 5 nm. This is likely because of a small size of water molecules with respect to the characteristic size of the confinement. More pronounced anisotropy due to the confinement effects may be expected for larger organic molecules in the same system of nanochannels.

TABLE I. Residence time,  $\tau_{res}$  (in ps), between jumps obtained from fitting the Lorentzian broadening parameter  $\Gamma(Q)$  using Eq. (3). Standard deviation values are shown in parentheses.

	$Q$ -perpendicular	$Q$ -parallel	Averaged between the two orientations
280 K	124.0 (9.8)	125.6 (15.0)	124.8 (12.4)
260 K	101.7 (7.2)	100.5 (7.1)	101.1 (7.2)
240 K	239.6 (7.9)	219.7 (8.2)	229.7 (8.1)

#### IV. CONCLUSION

In good agreement with the data available in the literature on the suppression of the water freezing point in confinement, our high-resolution QENS study of water dynamics in fully hydrated chrysotile asbestos fibers detected the freezing of water at about 237 K in the fiber channels with a characteristic size of 5 nm. The translational motion of water molecules, which slowed down by more than an order of magnitude compared to bulk water, was observed at 280, 260, and 240 K. The rotational component of the diffusion could not be observed, probably because it did not slow down enough from its bulk water values of 1–2 ps to be seen within the dynamic range of the backscattering spectrometer of  $\approx 20$  ps. The  $Q$  dependence of the quasielastic broadening was typical of a translational motion with a distribution of jump lengths, similar to that observed in bulk water. No major anisotropy in the relaxation time that would be indicative of translational motions of the water molecules primarily in the direction of the fiber axes was observed, probably because of a small size of water molecules compared to the characteristic length of confinement of 5 nm.

#### ACKNOWLEDGMENTS

The authors are grateful to D. Neumann and I. Peral for a critical reading of the manuscript. Utilization of the DAVE package for the data analysis is acknowledged. This work utilized facilities supported in part by the National Science Foundation under Agreement No. DMR-0086210. The work was partially supported by the RFBR (Grant Nos. 04-02-16550 and 03-02-16545) and INTAS (Grant No. 2001-0826).

- [1] H. Paoli, A. Méthivier, H. Jobic, C. Krause, H. Pfeifer, F. Stallmach, and J. Kärger, *Microporous Mesoporous Mater.* **55**, 147 (2002).
- [2] T. Takamuku, M. Yamagami, H. Wakita, Y. Masuda, and T. Yamaguchi, *J. Phys. Chem. B* **101**, 5730 (1997).
- [3] S. Takahara, M. Nakano, S. Kittaka, Y. Kuroda, T. Mori, H. Hamano, and T. Yamaguchi, *J. Phys. Chem. B* **103**, 5814 (1999).
- [4] F. Mansour, R. M. Dimeo, and H. Peemoeller, *Phys. Rev. E* **66**, 041307 (2002).
- [5] A. Faraone, L. Liu, C. Y. Mou, P.-C. Shih, C. Brown, J. R. D. Copley, R. M. Dimeo, and S.-H. Chen, *Eur. Phys. J. E* **12**, S59 (2003).
- [6] L. Liu, A. Faraone, C.-Y. Mou, P.-C. Shih, and S.-H. Chen, *J. Phys.: Condens. Matter* **16**, S5403 (2004).
- [7] M.-C. Bellissent-Funel, K. F. Bradley, S. H. Chen, J. Lal, and J. Teixeira, *Physica A* **201**, 277 (1993).
- [8] M.-C. Bellissent-Funel, S. H. Chen, and J.-M. Zanotti, *Phys. Rev. E* **51**, 4558 (1995).
- [9] J.-M. Zanotti, M.-C. Bellissent-Funel, and S. H. Chen, *Phys. Rev. E* **59**, 3084 (1999).
- [10] S. Mitra, R. Mukhopadhyay, K. T. Pillai, and V. N. Vaidya,



- Solid State Commun. **105**, 719 (1998).
- [11] D. J. Cebula, R. K. Thomas, and J. W. White, *Clays Clay Miner.* **29**, 241 (1981).
- [12] J. J. Tuck, P. L. Hall, M. H. B. Hayes, D. K. Ross, and C. Poinson, *J. Chem. Soc., Faraday Trans. 1* **80**, 309 (1984).
- [13] C. Poinson, H. Estrade-Szwarczopf, J. Conard, and A. J. Dianoux, *Physica B* **156-157**, 140 (1989).
- [14] M. Gay-Duchosal, D. Hugh Powell, R. E. Lechner, and B. Ruffle, *Physica B* **276-278**, 234 (2000).
- [15] J. Swenson, R. Bergman, and W. S. Howells, *J. Chem. Phys.* **113**, 2873 (2000).
- [16] J. Swenson, R. Bergman, and S. Longeville, *J. Chem. Phys.* **115**, 11299 (2001).
- [17] Y. Kuroda, S. Kittaka, S. Takahara, T. Yamaguchi, and M.-C. Bellissent-Funel, *J. Phys. Chem. B* **103**, 11064 (1999).
- [18] E. Mamontov, *J. Chem. Phys.* **121**, 9087 (2004).
- [19] For example, E. J. F. Whittaker, *Acta Crystallogr.* **6**, 747 (1953); **9**, 855 (1956); **9**, 862 (1956); **9**, 865 (1956).
- [20] K. Yada, *Acta Crystallogr.* **23**, 704 (1967).
- [21] K. Yada, *Acta Crystallogr., Sect. A: Cryst. Phys., Diffr., Theor. Gen. Crystallogr.* **27**, 659 (1971).
- [22] F. L. Pundsack, *J. Phys. Chem.* **60**, 361 (1956); **65**, 30 (1961).
- [23] Y. Kumzerov and S. Vakhruhev, in *Encyclopedia of Nanoscience and Nanotechnology*, edited by H. S. Nalwa (American Scientific Publishers, Los Angeles, 2004), Vol. 7, p. 811.
- [24] J. Teixeira, M.-C. Bellissent-Funel, S. H. Chen, and A. J. Dianoux, *Phys. Rev. A* **31**, 1913 (1985).
- [25] A. Meyer, R. M. Dimeo, P. M. Gehring, and D. A. Neumann, *Rev. Sci. Instrum.* **74**, 2759 (2003).
- [26] D. C. Steyler, J. C. Dore, and C. J. Wright, *J. Phys. Chem.* **87**, 2458 (1983).
- [27] M.-C. Bellissent-Funel, J. Lal, and L. Bosio, *J. Chem. Phys.* **98**, 4246 (1993).
- [28] K. Morishige and K. Nobuoka, *J. Chem. Phys.* **107**, 6965 (1997).
- [29] J. M. Baker, J. C. Dore, and P. Behrens, *J. Phys. Chem. B* **101**, 6226 (1997).
- [30] L. J. Smith, D. L. Price, Z. Chowdhuri, J. W. Brady, and M.-L. Saboungi, *J. Chem. Phys.* **120**, 3527 (2004).
- [31] P. A. Egelstaff, *An Introduction to the Liquid State* (Academic Press, London, 1967).
- [32] K. S. Singwi and A. Sjölander, *Phys. Rev.* **119**, 863 (1960).
- [33] Unlike  $\tau_{res}$ , which is defined by the quasielastic broadening measured at larger  $Q$  values, the mean square jump distance is determined from the data at small  $Q$  values. In our fitting, poor quality of the data at low  $Q$  results in very large errors for  $\langle r^2 \rangle$ , which makes the values of  $\langle r^2 \rangle$  determined from the fitting highly unreliable.